

## Temperature-dependent Raman spectra and anomalous Raman phenomenon of highly oriented pyrolytic graphite

PingHeng Tan, YuanMing Deng, and Qian Zhao

National Laboratory for Superlattices and Microstructures, P.O. Box 912, Beijing 100083, People's Republic of China

(Received 21 April 1998)

The Stokes and anti-Stokes Raman spectra of the pristine and ion-implanted highly oriented pyrolytic graphite (HOPG) are reported. For all Raman bands, noticeable frequency shifts are observed in the different temperature of samples. The anomalous Raman phenomenon (ARP) indicates that some modes occurring on the Stokes and anti-Stokes sides have different frequencies for HOPG. The data suggest that the ARP is closely related with the excitation wavelength ( $\lambda$ ) dependence of Raman bands of the graphite. According to the temperature effect and the ARP, we assign and verify some modes of HOPG, and predict some new results. [S0163-1829(98)08733-5]

### I. INTRODUCTION

The Raman spectra of graphite materials are known to reflect their structures very sensitively, and the relation between the spectra and structures has been well discussed.<sup>1-10</sup> The technique of ion implantation provides a method for artificially producing disordered regions of various sizes and it is applied in several studies.<sup>4,5</sup> The carbon materials have strong temperature effect.<sup>11,12</sup> It is expected that the ion-implanted samples have stronger temperature effect, but there are few reports about it for the ion-implanted highly oriented pyrolytic graphite (HOPG). For a reciprocal system by symmetry, it is well known that the same Raman modes occurring on the Stokes and anti-Stokes sides have the same frequencies according to the Raman theory that have been proved by many experiments. However, we find that it is not the case for HOPG. Some modes of the pristine and ion-implanted HOPG occurring on the Stokes and anti-Stokes sides have different frequencies. In this paper, we study the Stokes and anti-Stokes Raman spectra of the pristine and ion-implanted HOPG, and report this anomalous Raman phenomenon (ARP) carefully.

### II. EXPERIMENT

Samples of HOPG are the standard sample for achieving an atomic image of a graphite layer in a scanning tunnel microscope system (Park Scientific Instrument, U.S.A.). Some of the samples have been implanted with carbon (<sup>12</sup>C) ions at ambient temperatures (CHOPG) with fluence of  $1.0 \times 10^{14}$  ions/cm<sup>2</sup> and at an accelerating voltage of 100 keV. The ion beam was directed normal to the graphite *c* face.

The Raman spectra of pristine and ion-implanted HOPG's are recorded by the Dilor Super Labram with a typical resolution of  $1-2$  cm<sup>-1</sup> in backscattering geometry at room temperature. The system consists of a holographic notch filter for Rayleigh rejection and a microscope with an 100 $\times$  objective lens (numerical aperture=0.9), allowing a spatial resolution of less than 2  $\mu$ m. The sources are an Ar<sup>+</sup> laser at 488.0 and 514.5 nm (the laser power arrived at the samples in the range 2-100 mW), and a He-Ne laser at 632.8 nm with a typical laser power of 35 mW. The temperatures

of the samples are determined by measuring the relative intensities of Stokes and anti-Stokes Raman lines of 1582 cm<sup>-1</sup>.<sup>12,13</sup> All Raman lines are calibrated by a Ne lamp at the same experiment condition, and peak parameters are obtained by least-squares fitting Lorentzian line shapes to the measured spectra.

### III. RESULTS AND DISCUSSION

Monocrystalline graphite belongs to the  $D_{6h}$  symmetry group;<sup>1</sup> the irreducible representation for the Brillouin-zone center optical modes is given by

$$\Gamma_{\text{opt}} = 2E_{2g}(R) + E_{1u}(IR) + 2B_{2g} + A_{2u}(IR).$$

The  $2E_{2g}$  modes are Raman active. HOPG shows these  $2E_{2g}$  modes at 42 and 1582 (G) cm<sup>-1</sup>, respectively.<sup>2,3</sup> In addition, there are two extra first-order lines at  $\sim 1360$  and 1620 cm<sup>-1</sup> for ion-implanted HOPG and microcrystalline graphite,<sup>2,4-8</sup> which have been interpreted as fundamentals corresponding to the high density of phonon states on the basis of the wave-vector selection-rule relaxation that results from finite-crystal size effects and defects. Those two modes are often designated as the *D* mode and *D'* mode. In the region of higher-order Raman spectra, four distinct lines at  $\sim 2440$ ,  $\sim 2720$  (*2D*),  $\sim 3240$  (*2D'*), and  $\sim 4320$  (*2D+G*) cm<sup>-1</sup> are exhibited in HOPG (Refs. 5-9) and an extra line  $\sim 2950$  (*D+G*) cm<sup>-1</sup> is shown in ion-implanted HOPG.<sup>2,4,5</sup> Those Raman bands have been observed in the Raman spectra of HOPG and CHOPG excited with 514.5 nm (Fig. 1). For the CHOPG, there exists a Raman band of 1084 cm<sup>-1</sup> (marked as *T* for convenience) that is not observed in the HOPG. This band is considered to be fundamental, which is attributed to the features in the density of states. At the same time, there is a doublet at 1352 and 1370 cm<sup>-1</sup> in the position of  $\sim 1360$  cm<sup>-1</sup> (*D*) (Ref. 8) and a doublet at 2693 and 2728 cm<sup>-1</sup> in the position of overtone of *D* mode at  $\sim 2730$  cm<sup>-1</sup> (*2D*); we designate the doublet at 1352 and 1370 cm<sup>-1</sup> as *D*<sub>1</sub> and *D*<sub>2</sub>, and its overtone as *2D*<sub>1</sub> and *2D*<sub>2</sub>. According to the previous calculation of the phonon-dispersion relation and phonon density of states for the graphite,<sup>1,14,15</sup> the mode 1084 cm<sup>-1</sup> is probably associated

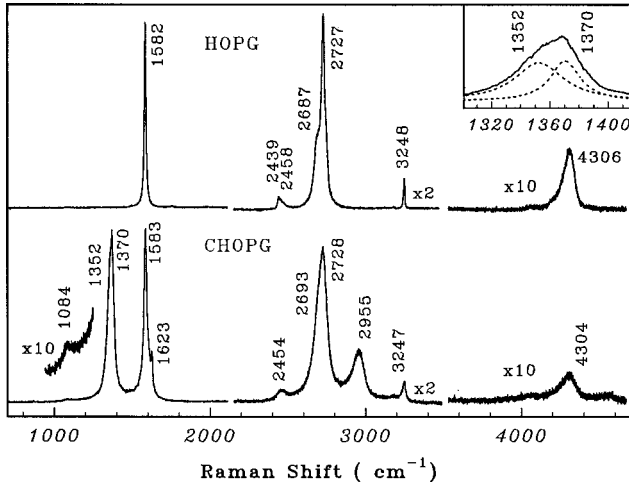


FIG. 1. Raman spectra of HOPG and CHOPG excited by 514.5 nm with laser power of 2 mW at the sample. The inset shows the doublet structure of  $D$  mode.

with contributions from regions near the  $K$  point of the Brillouin-zone boundary (for example, see Fig. 2 in Ref. 14), and becomes Raman active due to the selection-rule relaxation resulting from defects. For the  $D$  doublet, we assign its low-energy side  $D_1$  that mainly comes from the  $K$  point and high-energy side  $D_2$  that mainly comes from the  $M$  point. This assignment agrees with the calculation of a second-order Raman cross section by Al-Jishi and Dresselhaus.<sup>15</sup> The assignment of other observed peaks in Fig. 1 follows that of Ref. 7.

The Raman spectra of CHOPG and HOPG excited by 514.5 nm with different laser power are shown in Fig. 2. Table I summarizes the frequencies of Raman lines and the frequency shifts of the same Raman peaks between the two spectra excited with different laser power. Compared with the Raman spectrum of CHOPG in Fig. 1, the sample is annealed due to absorbing the energy of the laser; the degree of laser annealing is even comparable to annealing at temperature 950 °C for 0.5 h.<sup>5</sup> After laser annealing, the intensity of  $T$  is too weak to be identified, and as is also the case with that of the  $D$  mode which indicates the disorder of the samples is much decreased. However,  $D$  and  $2D$  modes show doublet structures clearly, and the line of  $\sim 2454$  cm<sup>-1</sup> of unannealed CHOPG in Fig. 1 shows a clear doublet at 2440 and 2460 cm<sup>-1</sup>. We assign these two doublet peaks to  $T+D_1$  and  $T+D_2$  from the frequency match of these combination modes. This assignment is consistent with that of

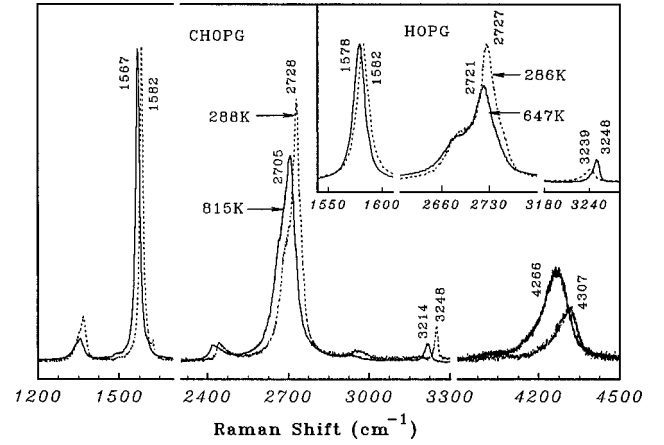


FIG. 2. Raman spectra of CHOPG and HOPG excited with 514.5 nm while laser power at the sample increased to 100 mW from 2 mW (the solid lines) and then decreased to 2 mW (the dashed lines).

$\sim 2450$  cm<sup>-1</sup> in the graphite from frequency match and the excitation wavelength ( $\lambda$ ) dependence.<sup>7</sup> For HOPG, although the  $D$  doublet and  $T$  mode are forbidden due to the selection rule, the doublet of  $\sim 2450$  and  $\sim 2720$  cm<sup>-1</sup> should be designed as  $T+D_1$ ,  $T+D_2$  modes and  $2D_1$ ,  $2D_2$  modes, respectively.

According to the relative intensities of Stokes and anti-Stokes Raman lines of  $G$  mode, we can calculate that the temperatures of CHOPG and HOPG are 815 and 647 K when the laser power is increased to 100 mW, and then decrease to about room temperature when the laser power decreases to 2 mW. Noticeable frequency shifts are observed for all the Raman bands during this process. This indicates that HOPG and CHOPG have strong temperature effects. The temperature dependence of higher-order bands follows that of the fundamentals and satisfies the sum rule. For example, the frequency shift of the  $2D+G$  mode ( $\sim 41$  cm<sup>-1</sup>) between two different temperatures for CHOPG is the sum of that of the  $2D$  mode ( $\sim 23$  cm<sup>-1</sup>) and  $G$  mode ( $\sim 15$  cm<sup>-1</sup>) or that of  $D+G$  mode ( $\sim 29$  cm<sup>-1</sup>) and  $D$  mode ( $\sim 11$  cm<sup>-1</sup>). So, according to the temperature dependence of Raman modes, we can verify the assignment of higher-order Raman modes of HOPG.

If we define the temperature coefficient  $\chi$  of the  $G$  mode as the frequency shift of the  $G$  mode when the temperature of the sample increases 1 K, then,  $\chi_{\text{HOPG}}=0.028$  cm<sup>-1</sup>/K and  $\chi_{\text{HOPG}}=0.011$  cm<sup>-1</sup>/K. The HOPG has a weaker tempera-

TABLE I. The Raman peaks of HOPG and CHOPG excited by 514.5 nm with different laser power. The temperature labeled under  $\omega$  is the calculated temperature of the sample.  $\delta\omega$  is the Raman shifts of the same Raman peaks between two Raman spectra with different laser power.

Assignment	$D_1$	$D_2$	$G$	$D'$	$T+D_1$	$T+D_2$	$2D_1$	$2D_2$	$D+G$	$2D'$	$2D+G$
HOPG											
$\omega_{647\text{K}}/\text{cm}^{-1}$			1578		2433	2452	2680	2720		3239	4294
$\omega_{286\text{K}}/\text{cm}^{-1}$			1582		2439	2458	2687	2727		3248	4306
$\delta\omega/\text{cm}^{-1}$			4		6	6	7	7		9	12
CHOPG											
$\omega_{815\text{K}}/\text{cm}^{-1}$	1339	1357	1567	1606	2422	2443	2668	2705	2930	3214	4266
$\omega_{288\text{K}}/\text{cm}^{-1}$	1350	1368	1582	1623	2440	2460	2689	2728	2959	3248	4307
$\delta\omega/\text{cm}^{-1}$	11	11	15	17	18	17	21	23	28	34	41

ture dependence due to higher thermal conductivity and a lower thermal expansion coefficient. However, the sample absorbs laser energy and expands easily due to the lower thermal conductivity that is caused by the shorter crystal planar domain size<sup>16</sup> when there exists defects and an impurity such as CHOPG. The thermal expansion induces a longer C-C distance and a downshift in the C-C stretching frequency.

The intensity of anti-Stokes Raman scattering  $I_{AS}$  is related to the temperature  $T$  of the sample sensitively,

$$I_{AS} \propto (\omega_L + \omega)^4 / [\exp(\hbar\omega/kT) - 1],$$

where  $\omega_L$  and  $\omega$  are the frequencies of the excitation laser and photon, respectively. Higher temperature of the samples is advantageous when observing the anti-Stokes Raman scattering. Because it is easy to increase the temperature of the ion-implanted HOPG by absorbing the energy of the laser, the anti-Stokes Raman scattering can be measured easily, including the  $2D+G$  mode whose frequency is up to  $\sim 4320 \text{ cm}^{-1}$ . It has been observed that modes occurring on the Stokes and anti-Stokes sides had different frequencies in the antiparallel antiferromagnet, but this comes from the fact that an antiparallel layer is a *truly nonreciprocal system* by symmetry.<sup>17</sup> So, the modes occurring on the Stokes and the anti-Stokes sides are *not the same modes*. For a reciprocal system by symmetry, different frequencies between some of *the same Raman modes* of the HOPG occurring on the Stokes and anti-Stokes sides are observed in our experiment. For example,  $\omega_S(2D) = 2735 \text{ cm}^{-1}$ , but  $\omega_{AS}(2D) = -2761 \text{ cm}^{-1}$ . The frequency shift between  $\omega_S(2D)$  and  $\omega_{AS}(2D)$  is even on the same magnitude of the half width at half maximum of the  $2D$  mode.

Figure 3 shows the Stokes and anti-Stokes Raman spectra of CHOPG, HOPG, and diamond excited by 488.0 nm. All spectra on the same picture are labeled with the same scale for convenient to compare. It does not show *frequency shifts between Stokes and anti-Stokes lines* (FSSA) of  $G$ ,  $D'$ , and  $2D'$  modes for CHOPG and that of the peak of  $\sim 1332 \text{ cm}^{-1}$  for diamond in the range of experimental precision. However, obvious FSSA can be found from the other modes. We define the FSSA of the  $M$  mode as  $\Delta(M) = (|\omega_S(M)| - |\omega_{AS}(M)|)$ , where  $\omega_S$  and  $\omega_{AS}$  are the frequencies of Stokes and anti-Stokes, respectively. Then,  $\Delta(D_1) = -6 \text{ cm}^{-1}$ ,  $\Delta(D_2) = -7 \text{ cm}^{-1}$ ,  $\Delta(T+D_1) = 21 \text{ cm}^{-1}$ ,  $\Delta(T+D_2) = 22 \text{ cm}^{-1}$ ,  $\Delta(2D_1) = -25 \text{ cm}^{-1}$ ,  $\Delta(2D_2) = -26 \text{ cm}^{-1}$ ,  $\Delta(D+G) = -13 \text{ cm}^{-1}$ , and  $\Delta(2D+G) = -45 \text{ cm}^{-1}$ . So, the FSSA of CHOPG can be divided into three classes: compared with that of anti-Stokes lines, the Raman frequencies of Stokes lines of CHOPG are upward shifted ( $T+D_1$  and  $T+D_2$ ), insensitive ( $G$ ,  $D'$ , and  $2D'$ ) and downward shifted ( $D_1$ ,  $D_2$ ,  $2D_1$ ,  $2D_2$ ,  $D+G$ , and  $2D+G$ ). This is one of the anomalous phenomena of Raman spectra of HOPG. At the same time, the data also suggest that the FSSA of overtones or combinations do not obey the sum rules of their fundamentals in contrast to the temperature dependence. For example,  $\Delta(2D_1)$  ( $= -25 \text{ cm}^{-1}$ ) is not twice as much as  $\Delta(D_1)$  ( $= -6 \text{ cm}^{-1}$ ). The same results are found in the HOPG as well as in the ion-implanted HOPG [see Fig. 3(b)]. This indicates that the ARP is mainly dominated by the structure feature of the graphite layer, and

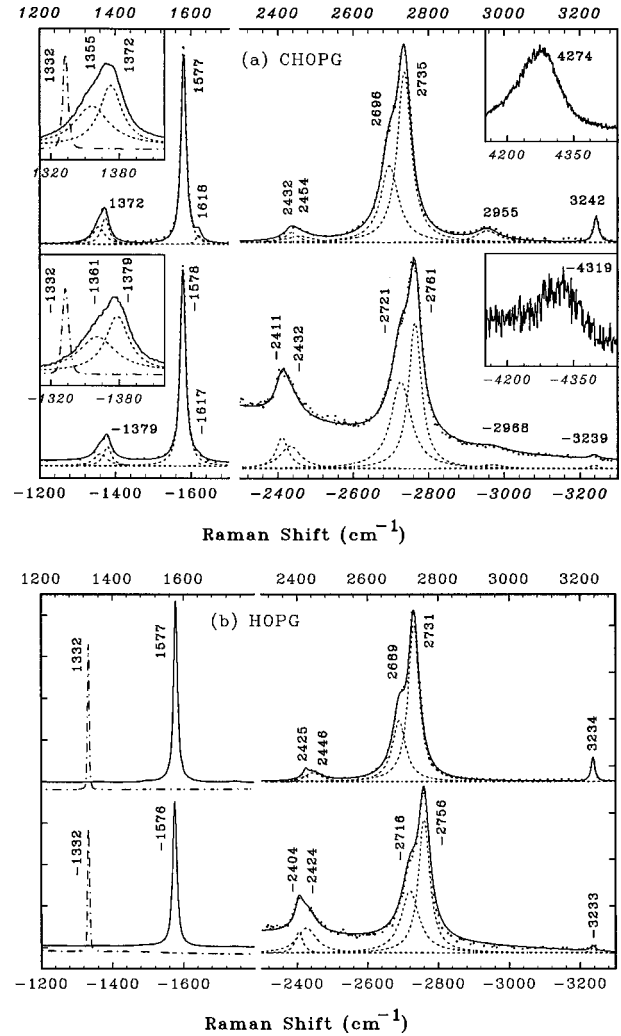


FIG. 3. The Stokes and anti-Stokes Raman spectra excited by 488.0 nm: (a) CHOPG. The left insets show Raman spectra of the doublet  $D$  mode and the right insets show those of  $2D+G$  mode at the higher temperature of sample. (b) HOPG. The dashed lines show the peaks used to fit the spectra, the solid lines are the fitted results, and the dashed-dotted lines show the spectra of diamond.

has little relationship with the degree of disorder in spite of the important role that disorder plays in the spectra. It is reasonable to predict that the ARP could be observed in the samples with small crystalline domain sizes such as graphite fibers, carbon nanotubes, and graphite intercalation compounds.

Because the spectra of CHOPG have strong temperature dependence, we measured the Stokes and anti-Stokes Raman spectra of CHOPG excited by 514.5 nm at two different temperatures (816 and 567 K). They are shown in Fig. 4. At 816 K,  $\Delta(2D+G) = -44 \text{ cm}^{-1}$  is observed. With the temperature increasing, the Stokes and anti-Stokes lines shift by almost the same frequency. So, the FSSA is almost insensitive to the temperature of the sample although the frequencies of Stokes and anti-Stokes are notably shifted with the changing of the sample temperature. The spectra of CHOPG excited by 632.8 nm are also shown in Fig. 4 and  $\Delta(T) = 14 \text{ cm}^{-1}$  is measured. Since the laser power of 632.8 nm is relatively small and the laser annealing is weak, the intensity of the  $T$  mode is stronger than that of larger laser power, and

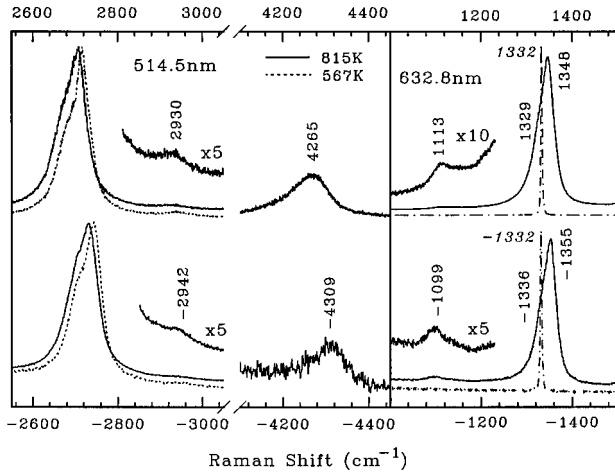


FIG. 4. The Stokes and anti-Stokes Raman spectra of CHOPG excited by 514.5 nm at two different sample temperatures and excited by 632.8 nm. The dashed-dotted line shows the spectra of diamond.

it is easy to obtain the anti-Stokes line of the  $T$  mode. Because the FSSA is almost insensitive to the temperature of the samples, all the data about the FSSA of HOPG and CHOPG excited with difference sources are summarized in Table II.

In order to exclude the influence of temperature, the Raman spectra of HOPG and CHOPG excited by the laser power of 2–5 mW at the sample is measured; in this case the temperature of all samples is about room temperature, and Raman spectra of CHOPG are obtained after laser annealing with laser power as high as can be obtained, for example, 100 mW for 514.5- and 488.0-nm excitation, and 10 mW for 632.8-nm excitation. The frequencies of all those bands are also summarized in Table II. The  $\lambda$  dependence of all Raman bands of HOPG and CHOPG is the same as that of pyrolytic graphite:<sup>7</sup> with the increase of excitation wavelength ( $\lambda$ ), the frequencies of Stokes and anti-Stokes bands of CHOPG and HOPG are upward shifted ( $T$ ,  $T+D_1$ , and  $T+D_2$ ), insensitive ( $G$ ,  $D'$ , and  $2D'$ ), and downward shifted ( $D_1$ ,  $D_2$ ,  $2D_1$ ,  $2D_2$ ,  $D+G$ , and  $2D+G$ ) separately, and

the Stokes and anti-Stokes lines shift at nearly the same frequency. Therefore, the FSSA are almost insensitive to the excitation wavelength ( $\lambda$ ) although the frequencies of Stokes and anti-Stokes shift obviously when the excitation wavelength is changed. This also affirms that ARP does not arise from the error of the instrument. Furthermore, because the Raman frequencies of Stokes lines of HOPG and CHOPG are upward shifted ( $T$ ,  $T+D_1$ , and  $T+D_2$  modes), insensitive ( $G$ ,  $D'$ , and  $2D'$  modes), and downward shifted ( $D_1$ ,  $D_2$ ,  $2D_1$ ,  $2D_2$ ,  $D+G$ , and  $2D+G$  modes) compared with that of anti-Stokes lines, this indicates that the shifts of the frequencies between Stokes and anti-Stokes lines are in concord with the shifts of the corresponding Raman lines while increasing the excitation wavelength. This suggests that ARP has close relationship with the  $\lambda$  dependence of the Raman spectra of HOPG. With regard to this point, we firmly believe that the ARP and the  $\lambda$  dependence of HOPG have the same origin, although the  $\lambda$  dependence of Raman lines is too complicated to be explained by the existing calculations.<sup>7</sup>

According to the calculated phonon-dispersion relations and the phonon density of states,<sup>6,14,15</sup> a high density of states is associated with the highest phonon branch with a large contribution arising from modes near the Brillouin-zone boundary, such as the  $T$  and  $D$  modes. However, for the highest-lying branch, the maximum phonon frequency does not occur at the zone center but at a lower symmetry point  $\Sigma$  along the  $\Gamma$ - $M$  axis, which is designed as the  $D'$  mode. The  $T$  and  $D$  modes and their combinations such as the  $T+D$ ,  $2D$ ,  $D+G$ , and  $2D+G$  modes exist in the ARP and strong  $\lambda$  dependence, but the  $D'$  mode, zone-center optical lattice mode such as the  $G$  mode, and the overtone of the  $D'$  mode do not exist in the ARP and the  $\lambda$  dependence. Therefore, as well as the  $\lambda$  dependence of Raman modes of graphite,<sup>8</sup> the ARP of the  $T$  and  $D$  modes and their combination modes may be related to the dispersion of  $T$  and  $D$  modes at the Brillouin-zone edge. We can use the ARP for distinguishing whether the Raman mode of graphite material can be attributed to features in the density of states near the Brillouin-zone boundary or not, and for determining whether the combination modes of graphite material consists of the fundamentals that exist in the ARP such as the  $T$  and  $D$  modes.

TABLE II. Frequency difference between Stokes and anti-Stokes lines of HOPG and CHOPG excited by 488.0, 514.5, and 632.8 nm is defined as  $\Delta = (|\omega_S| - |\omega_{AS}|)$ . The blank cells indicate that those modes are silent or their positions are not easily determined due to weak intensity and low signal-to-noise ratio. The frequencies of all modes in the table are obtained when the temperature of HOPG and laser-annealed CHOPG are at the room temperature (see the text) except that of the  $T$  mode of CHOPG that is obtained before annealing.

Assignment		$T$	$D_1$	$D_2$	$G$	$D'$	$T+D_1$	$T+D_2$	$2D_1$	$2D_2$	$D+G$	$2D'$	$2D+$		
													$G$		
HOPG	488.0 nm	$\omega/\text{cm}^{-1}$			1582		2433	2452	2696	2738		3247	4318		
		$\Delta\omega/\text{cm}^{-1}$			1		21	22	-27	-25		1			
	514.5 nm	$\omega/\text{cm}^{-1}$			1582		2439	2458	2687	2727		3248	4306		
		$\Delta\omega/\text{cm}^{-1}$			1		22	19	-25	-26		2			
CHOPG	488.0 nm	$\omega/\text{cm}^{-1}$	1072	1359	1376	1582	1624	2435	2456	2703	2742	2964	3250	4320	
		$\Delta\omega/\text{cm}^{-1}$		-6	-7	-1	1	21	22	-25	-26	-13	3	-45	
	514.5 nm	$\omega/\text{cm}^{-1}$	1084	1350	1368	1582	1623	2440	2460	2689	2728	2959	3248	4307	
		$\Delta\omega/\text{cm}^{-1}$		-7	-6	1	-1	21	19	-28	-27	-12	2	-44	
	632.8 nm	$\omega/\text{cm}^{-1}$	1115	1331	1350	1583	1623		2465		2648	2689	2936	3246	4262
		$\Delta\omega/\text{cm}^{-1}$	14	-7	-7	1	0		19		-28	-27	-12	-2	

It is well known that carbon may form different types of bonding, for example,  $sp^3$  bonding in crystalline diamond or  $sp^2$  bonding in graphite. We do observe the ARP of the  $D$  mode at  $\sim 1350\text{ cm}^{-1}$  for the graphite, but we do not observe the ARP of the  $1332\text{-cm}^{-1}$  line for the diamond. Therefore, the ARP may be a powerful tool for distinguishing between the  $sp^2$  and  $sp^3$  bonding of carbon material.

#### IV. SUMMARY

The Stokes and anti-Stokes Raman spectra of the pristine and ion-implanted HOPG are reported. Noticeable frequency shifts are observed for all those Raman bands with different power of laser excitation. It is interpreted as a longer C-C distance and a downshift in the C-C stretching frequency that are induced by the thermal expansion due to the absorbed laser energy. The ARP where some modes of the pristine and ion-implanted HOPG occurring on the Stokes and anti-Stokes sides have different frequencies is reported. The peculiar features of the ARP are found to be as follows: (a) the Raman frequencies of Stokes lines of CHOPG are upward shifted ( $T$  and  $T+D$  modes), insensitive ( $G$ ,  $D'$ , and  $2D'$  modes), and downward shifted ( $D$ ,  $2D$ ,  $D+G$ , and  $2D$

+ $G$  modes) relative to that of anti-Stokes lines, (b) the FSSA are almost insensitive with the wavelength of laser excitation and the temperature of samples, (c) the FSSA of higher-order bands do not follow that of the fundamentals. The data suggest that ARP is not related to the disorder of samples, but has a close relationship with the  $\lambda$  dependence of the graphite Raman modes. This indicates that the ARP and the  $\lambda$  dependence of the graphite have the same origin.

Although the origin of those peculiar FSSA of HOPG has not been as well understood as the  $\lambda$  dependence of Raman lines, it is useful for the assignment and verification of the first-order and higher-order modes. It is necessary to investigate Stokes and anti-Stokes Raman spectra in a variety of graphite materials with higher signal-to-noise ratio and higher resolution than the present work to further reveal the origin of the ARP.

#### ACKNOWLEDGMENTS

It is our pleasure to thank Professor ZhaoPing Wang, Professor HouZhi Zheng, Professor GuoHua Li, and Professor HeXiang Han for their helpful discussions.

- 
- <sup>1</sup>M. S. Dresselhaus and G. Dresselhaus, in *Light Scattering in Solids III*, edited by M. Cardona and G. Güntherodt (Springer, Berlin, 1982).
- <sup>2</sup>L. J. Brillson, E. Burnstein, A. A. Maradulin, and T. Stark, in *Proceedings of the International Conference on Semimetals and Narrow Gap Semiconductors*, edited by D. L. Carter and R. T. Bate (Pergamon, New York, 1971).
- <sup>3</sup>K. Sinha and J. Menendez, *Phys. Rev. B* **41**, 10 845 (1990).
- <sup>4</sup>B. S. Elman, M. Shayegan, M. S. Dresselhaus, H. Mazurek, and G. Dresselhaus, *Phys. Rev. B* **25**, 4142 (1982).
- <sup>5</sup>B. S. Elman, M. S. Dresselhaus, G. Dresselhaus, E. W. Maby, and H. Mazurek, *Phys. Rev. B* **24**, 1027 (1981).
- <sup>6</sup>R. J. Nemanich and S. A. Solin, *Phys. Rev. B* **20**, 392 (1979).
- <sup>7</sup>Y. Kawashima and G. Katagiri, *Phys. Rev. B* **52**, 10 053 (1995).
- <sup>8</sup>R. P. Vidano, D. B. Fischbach, L. J. Willis, and T. M. Loehr, *Solid State Commun.* **39**, 341 (1981).
- <sup>9</sup>P. H. Tan, S. L. Zhang, Kuo To Yue, F. M. Huang, Z. J. Shi, X. H. Zhou, and Z. N. Gu, *J. Raman Spectrosc.* **28**, 369 (1997).
- <sup>10</sup>F. Tuinstra and J. L. Koenig, *J. Chem. Phys.* **53**, 1126 (1970).
- <sup>11</sup>P. V. Huong, R. Cavagnat, P. M. Ajayan, and O. Stephan, *Phys. Rev. B* **51**, 10 048 (1995).
- <sup>12</sup>P. V. Huong, *Solid State Commun.* **88**, 23 (1993).
- <sup>13</sup>*Raman Spectroscopy Linear and Non Linear*, edited by J. Lascombe and P. V. Huong (Wiley, New York, 1982).
- <sup>14</sup>P. Lespade, R. Al-Jishi, and M. S. Dresselhaus, *Carbon* **20**, 427 (1982).
- <sup>15</sup>R. Al-Jishi and G. Dresselhaus, *Phys. Rev. B* **26**, 4514 (1982).
- <sup>16</sup>J. Heremans, I. Rahim, and M. S. Dresselhaus, *Phys. Rev. B* **32**, 6742 (1985).
- <sup>17</sup>P. Grünberg, R. Schreiber, Y. Pang, M. B. Brodsky, and H. Sowers, *Phys. Rev. Lett.* **57**, 442 (1986).